CLIMATE VARIABILITY AND LAND COVER CHANGE IMPACTS ON THE WATER BALANCE OF THE CARONÍ RIVER BASIN, VENEZUELA

Maria Dolores Delgado y Lelys Bravo de Guenni[1]
UNIVERSIDAD SIMÓN BOLÍVAR, CARACAS, VENEZUELA

1. INTRODUCTION

One of the main reasons to study the hydrological processes of the Caroní river basin, is the hydropower potential of this catchment, which provides 70% of the country's electrical energy. It also supplies all the energy for the industrial activity located in the Guayana region and to the transmission line going through the south-east of the country in Bolívar state. This transmission line attends the demand of the northern region of Brazil. It also supplies all the energy needed by the 2 million of inhabitants located north of the Caroní river (EDELCA, 2001). This analysis provides valuable information for the new development plans of the region and for the establishment of priority areas for the conservation of its water resources.

Most hydro electrical projects are planned for several decades and the basin is now under different stresses like population growth, land use and land cover change and climate variability and change. The stakeholders and planning managers need to understand the actual hydrological and ecological offer and the impacts of vegetation change and climate variability over the region water resources. Under the Millennium Assessment approach, it means to quantify the water related ecosystem services (Millennium Ecosystem Assessment, 2003) for human well being.

To understand the spatial distribution of the physical variables related to the water cycle (precipitation, evapotranspiration, soil moisture and runoff) conceptual water balance models are the main tool used at global and regional scales (Yates, 1997; Arnell, 1999; Vörösmarty et al., 1989, 1996, 1998; Döll et al., 2003). Most of these models calculate the surface water balance for each grid cell and might be coupled to water transfer models to calculate the horizontal water flow. The estimation of the potential evapotranspiration is usually an important problem since model results are highly sensitive to the methodology used.

This problem is also explored in this research.

Given the fragility of the forest ecosystem in this region, especially in the area of La Gran Sabana National Park, numerous studies have reported a potential substitution of the forest cover by savanna communities (Huber, 1986; Dezzeo, 1994; Kingsbury, 2001). This research explores the impacts of these changes on the components of the hydrological cycle. On another hand some studies have demonstrated the impacts of ENSO on the hydro-climatology of the region (Poveda and Mesa, 1997; Guenni et al., 2002; Cárdenas et al., 2003). This topic is also explored by applying the WBM proposed by Vörösmarty et al., (1989, 1998) under an El Niño typical condition.

2. STUDY AREA

The Caroní river basin is located at Bolívar state, South-east Venezuela between the 3°40' and 8°40' north latitude and 60°50' and 64°10' west longitude. It is formed by the Caroní and Paragua rivers and it covers an area of 95.000 km^2 (around 10% of the national territory) (Figure 1). This area includes important protected zones as Canaima National Park, La Paragua Forest Reserve, Ikabarú National Reserve and several National Monuments as the Tepuy mountains. The mean annual precipitation is about 2,800 mm with a complex spatial distribution. There is a north-south precipitation gradient going from 1,000 mm/yr at the confluence of the Caroní with the Orinoco river, up to over 4,000 mm/yr west of the Icabarú river. There is also an east-west gradient with 1,800 mm/yr at the south-east sector of La Gran Sabana region, up to more than 4,000 mm/yr south west of the Paragua catchment. Similarly, the complex altitudinal gradient generates strong temperature gradients with mean annual temperatures over 24°C close to the confluence with the Orinoco river up to 10°C at the top of the Tepuy mountains.

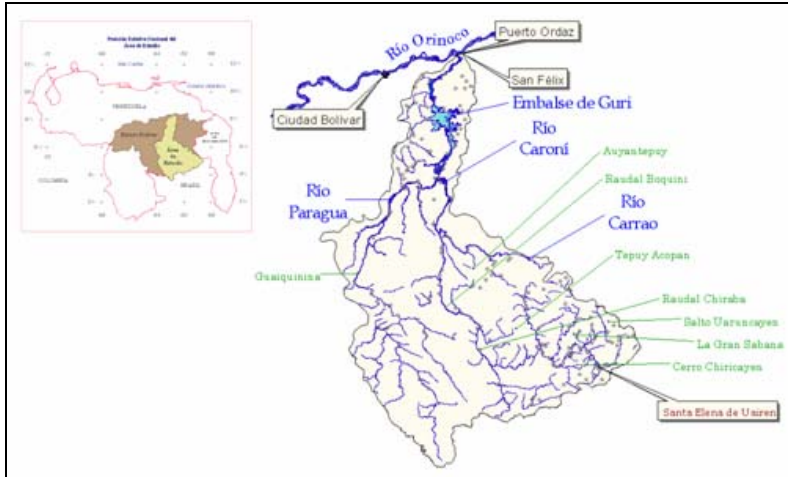[1] Corresponding Author: lbravo@usb.ve

Figure 1: Location of the Caroní river Basin

The Caroní river exhibits an average slope of 3,06 m/km along its way and the Paragua river presents an average slope of 0,91 m/km. These slope characteristics and relatively low sediments from the main tributaries, with runoff values of 5,000 m³/s, made this river the one with largest hydro electrical potential in Venezuela. Actually it produces 70% of the generated energy for national consumption (EDELCA, 2001). Table 2 shows the main characteristics of the three big catchment areas: Low Caroní, Upper Caroní and La Paragua.

The Caroní cachment is represented by a diverse group of vegetation communities as a result of the climate variability, complex landscape and soil characteristics, past climate changes and human activities. Seventy five per cent of the surface is covered by forests of different types (Huber,1986). Savannas are the second most dominant vegetation type, located mostly north and southeast of the catchment.

3. WATER BALANCE MODELING APPROACH

To model the components of the surface water balance, the WBM model developed by Thornwaite and Mather (1957) and later modified by Vörösmarty *et al.* (1989,1998) was used. This model applies a "bucket" approach to estimate runoff. When the soil reaches its water holding capacity, the runoff process takes place, otherwise soils recharge goes on. This model can be represented by the equation:

$$R = Pa - (Hs + Ea) \qquad (1)$$

Table 1. Regions of the Caroní river basin (EDELCA, 2001)

	Low Caroní	Upper Caroní	Paragua (Upper and Low)
Location	From the confluence with La Paragua river until the confluence with the Orinoco river	From the birth of the Caroní river at Kukenán tepuy, up to the confluence with La Paragua river at San Pedro de las Bocas.	From its birth at Marutaní tepuy until the confluence with the Caroní river
Approximate area	15,000 km2	47,000 km2	33,000 km2
Altitude difference	Between 270 and 6 masl*	2,800 and 270 masl	1,500 and 270 masl
Length	188 km	642 km	550 km

*: meters above sea level

where R is the total volume runoff, Pa is the precipitation, Hs is the soil water content, *Hs* represents soil water content changes between successive time steps and Ea is the actual evapotranspiration. This model is applied to each grid cell at a monthly time step (Figure 2). The snow compartment is disabled in the analysis. Through repeated application of the model it reaches an equilibrium state and model simulations begin at the end of the wet season when the soil is assumed to have reached its field capacity. A quasi-daily time step is adopted by disaggregating the monthly precipitation values to daily values. This is done by using the dependence between the number of wet days and the monthly totals calculated with a non-linear model between the probability of wet days and the total monthly rainfall. The parameters of this model are regionalized to account for the spatial variability of this relationship (Guenni, 2005, personal communication).

Soil water content (Hs) is determined for each grid cell from the interactions between the precipitation (Pa) and the potential evapotranspiration (Ep). When Pa exceeds Ep (wet months), Hs increases until it reaches the water holding capacity (Wc), which is determined by soil texture and root depth. When Ep exceeds Pa (dry months), Hs decreases according to a soil water loss function. Actual evapotranspiration (Ea) is set to Ep when precipitation is greater than Ep (wet months). Otherwise it is calculated as the potential evapotranspiration minus the changes in soil moisture. Unless the soil reaches its field capacity, all water will be used for soil water recharge. Otherwise exceeding water is used for groundwater

recharge and surface runoff. Model equations are presented in Appendix A.

The model was applied to a spatial window defined by coordinates 3º30' - 8º30' north latitude and, 60º30'- 64º30' west longitude with spatial resolution of 1 km x 1 km.

4. DATA DESCRIPTION

Several data sets are required to simulate the water balance components using the WBM model. These data sets were organized in the Geographical Information System (GIS) Idrisi 3.2 Release Two (Clark Labs., 1994-2002) and visualized in the ArcView GIS 3.2 system (ESRI, 1992-1999). The GHAAS-RGis 2.1 (Water System Analysis Group, UNH: 1994-2000) software was used to perform the water balance by composing all data sets into the same spatial resolution. This conversion was mostly accomplished with Idrisi 3.2.

The global Digital Elevation Model (GTOPO30) developed b the US Geological Survey (http://edcdaac.usgs.gov/gtopo30/gtopo30.asp) was used by sectioning the corresponding window for the Caroní basin. The digital river network was digitized and converted to a raster format from 8 charts developed by the Instituto Geográfico Simón Bolívar (Venezuela).

The hydro-climatological data was obtained from the Department of Environmental Management of the EDELCA Company, which is the main electricity production operator in the region. Data on precipitation,
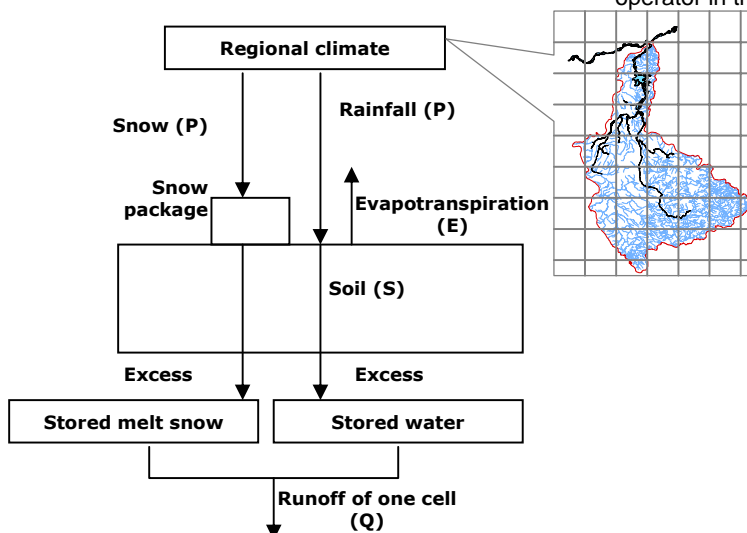

Figure 2. Water Balance representation at the grid scale (Adapted from Vörösmarty *et al.*, 1986)

maximum, minimum and mean air temperature, Pan evaporation, radiation, relative humidity, water discharge, and water levels at some locations were provided by EDELCA. Some of their records go back to 1958. A quality control processing was applied to these data sets and mean monthly and annual values of precipitation, maximum, minimum and mean air temperature were interpolated by using the ANUSPLIN software. Most of the point records correspond to the period 1980-2000. This software uses Laplacian Thin Plate Smoothing Splines (Hutchinson, 2002) for the spatial interpolation of climatic variables and has been applied widely around the world. Other climatic variables as wind velocity, radiation and vapor pressure data were only available at few locations and were not amenable for spatial interpolation. Different data sources were used to get these variables: wind velocity and atmospheric pressure were obtained from the Climate Research Unit data set (Hulme et al., 1999; New et al., 2002); while solar radiation was obtained from the Langley Research Center (Atmospheric Sciences Data center from NASA) (http://eosweb.larc.nasa.gov) at a resolution of 1° by 1°. All these data sets were resampled to the 1 km x 1 km resolution.

Vegetation data was obtained from the South-America Vegetation Map (Eva et al., 2002) and the window corresponding to the basin was sectioned from this data set. This map originally has more than 40 vegetation classes, but was reclassified into six categories: forest, savannas/shrubs, grasslands, crops, urban areas and water bodies/lakes. Soil texture was obtained from the soils map produced by CVG-TECMIN (1987). This map was digitized, rasterized

and reclassified into six soil texture categories: sandy (coarse), loam (medium), clay (fine), clay-loam (fine+medium), and sandy-loam (coarse+medium).

Potential evapotranspiration (ETP) can be estimated by several methods: Priestly and Taylor, McNaughton and Black, Penman, Penman- Montieth and Shuttleworth-Wallace. Several authors have compared these methodologies for different regions of the world (Federer et al., 1996); Vörösmarty et al, 1998; Fisher et al, 2005). Figure 3 shows the monthly mean ETP values calculated with the 5 methodologies. The Shuttleworth-Wallace method is a modification of the Penman-Montieth method, which accounts separately soil transpiration from soil evaporation. This method was selected because of its better estimation of the ETP for the water bodies (mean value of 81.3 mm/month). On average it does not overestimate or underestimate the mean monthly values and indirectly considers evaporation by vegetation interception. Given the dominant vegetation characteristics of the region this amount can not be underestimated.

As described in Vörösmarty et al. (1998) the soil water holding capacity defined as the field capacity minus the wilting point, is derived for each soil type. For each combination of soil texture and vegetation class, a root depth is estimated for each grid cell. For ETP estimations, the parameters required for each vegetation type (albedo, canopy height, maximum leaf area index, maximum leaf conductance, leaf width, soil surface roughness parameter, soil evaporation resistance) were adapted from Federer et al. (1996, 2003).
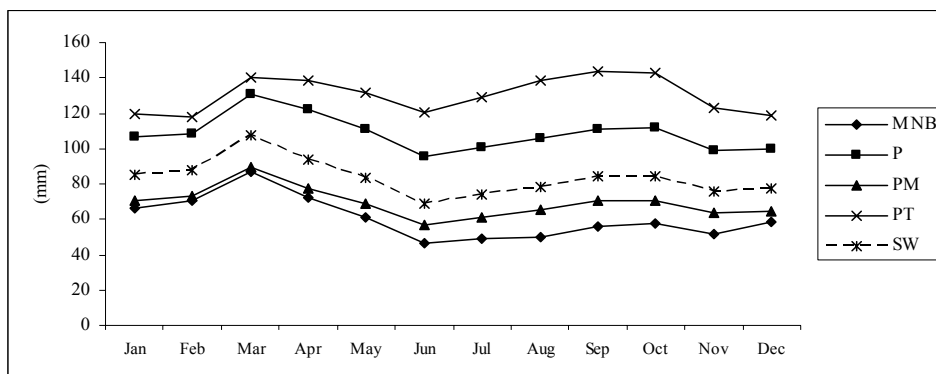

Figure 3: Mean monthly values of the Potential Evapotranspiration estimated by different methods (MNB:McNaughton-Black; P: Penman; PM: Penman-Monteith; PT: Priestly-Taylor; SW: Shuttleworth-Wallace).

Figure 3. Mean monthly values of the Potential Evapotranspiration estimated by different methods (MNB:McNaughton-Black; P: Penman; PM: Penman-Monteith; PT: Priestly-Taylor; SW: Shuttleworth-Wallace).

5.   RESULTS

5.1 *Mean annual water balance*

Table 2 shows a summary of the mean, maximum and minimum values for precipitation, actual evapotranspiration, soil moisture and surface runoff in mm.

Figure 4 shows the spatial variation of the four components of the water balance described in Table 2.There is a north-south and east-west decreasing precipitation gradient in the region as a consequence of the Inter-tropical Convergence Zone (ITZ) and the northeasterly winds. There is also a local precipitation increase with the presence of the Tepuys mountains, however there is not a clear relationship of precipitation with altitude and the complex topography of the

region plays a very important role in determining local precipitation variability (Schmidt, 2004).

The soil water content shows three important regions: one of low variability where low soil moisture is the result of low precipitation (northern region and La Gran Sabana region); a second region where other biogeophysical factors than rainfall limit the amount of soil moisture; and a third region in where soil moisture is not limited by precipitation values and the soil reaches its field capacity. The general distribution of the actual evapotranspiration follows closely the spatial distribution of precipitation. In a large proportion of the catchment, precipitation is high enough to satisfy the evaporative demands. As a

Table 2. Mean annual estimates of WBM

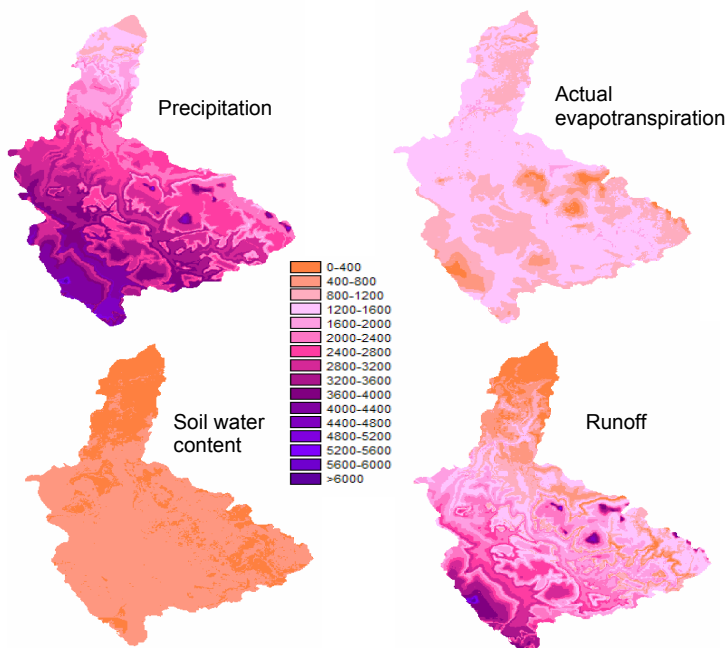| Estimated Values	Precipitation (mm)	Soil Moisture (mm)	Actual Evapotranspiration (mm)	Surface Runoff (mm)
Maximum	6361.58	582.80	1676.28	6360.58
Mean	2870.99	429.76	1214.66	1656.33
Minimum	483.42	0.00	0.12	0.00

Figure 4: Mean annual values (in mm) of the components of the hydrological cycle for the Caroní river basin

consequence ETA equals ETP for many grid cells. Surface runoff represents 58% of the annual precipitation, with the highest values (>4000 mm/year) occurring in La Paragua and at the top of the Tepuy mountains. The lowest values occur at the Low Caroní and La Grab Sabana region. The forest areas represent the largest vegetation cover type (75%) and get the maximum mean annual precipitation values with the highest proportion of surface runoff (59.9%).

A summary of the catchment response to precipitation is given in Figure 5 through the runoff coefficient. Whilst precipitation reaches a level of 1000 mm, runoff values increase abruptly indicating a rapid recharge of the soil moisture. After 1000 mm the runoff coefficient is approximately linear indicating that soil runoff equals precipitation minus actual evapotranspiration. The runoff coefficient reaches values close to 1 when precipitation is above 6000 mm, which it only occurs at few locations.

5.2 *Mean monthly water balance*

The mean monthly runoff values for the catchment are presented in Figure 6. Soil moisture and actual evapotranspiration show very homogeneous patterns across the catchment (figures not shown) and during the year, while surface runoff follows very closely the spatial and seasonal precipitation patterns of the region. This can be easily explained because of the high precipitation values which are able to keep high soil water content, and as a consequence, the resulting runoff is mainly the difference between precipitation and actual evapotranspiration.

The homogenous patterns of soil water content and actual evapotranspiration are shown in Figure 7, in contrast with the highly seasonal patterns of precipitation and surface runoff. For most of the year actual evapotranspiration equals the potential evapotranspiration (see Figure 8), since the high precipitation values can satisfy the evaporative demand and keep the soils close to field capacity. Only a slight decrease in soil moisture occurs during the driest months between February and April.
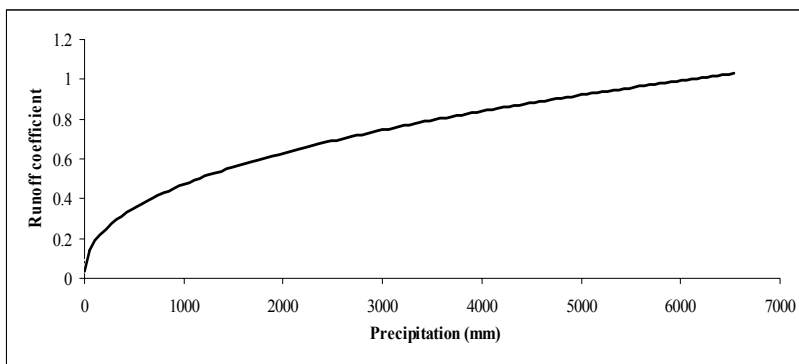

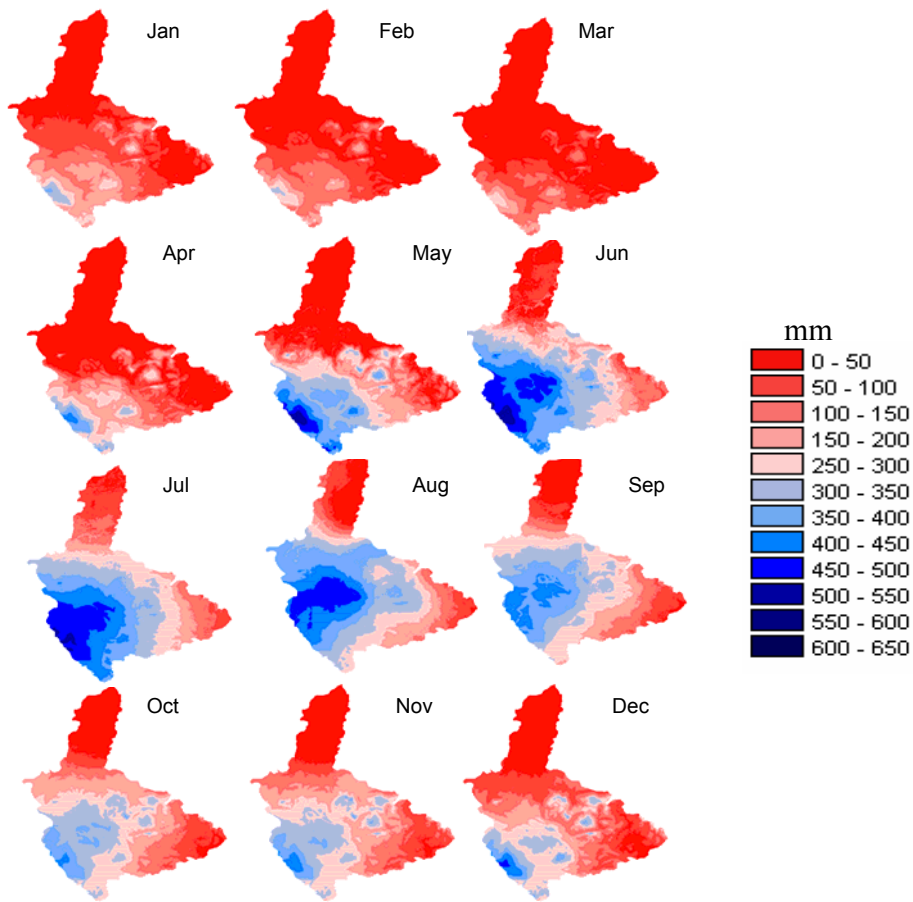**Figure 5**: Expected runoff coefficient for the Caroní river basin

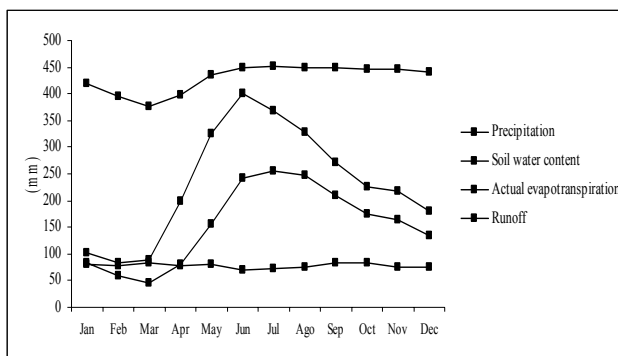**Figure 6**. Mean monthly surface runoff at the Caroní river basin.

Figure 7. Mean monthly distribution of the components of the hydrological cycle
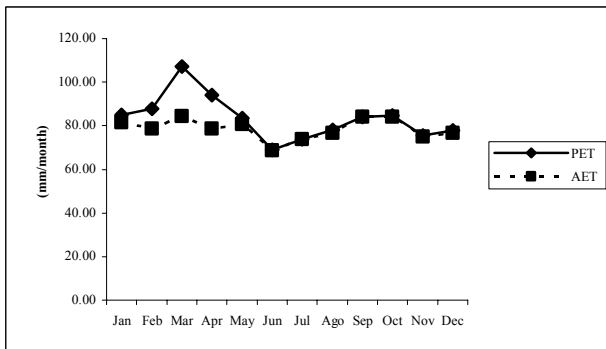
Figure 8. Mean values of potential evapotranspiration (PET) and actual evapotranspiration (AET)

5.3 Impacts of land cover on the components of the hydrological cycle

To evaluate the impacts of land cover on the seasonal variability of the components of the hydrological cycle, two grid cells were selected: one with forest cover and one with savanna cover. The seasonal variation of the WBM model outputs at both grid cells was examined. Care was taken to select grid cells with the same soil texture (loam) and neighboring cells with same vegetation cover. The results are shown in Figures 9 and 10.

From these two figures it is clear that on savannas regions since precipitation is lower than on forested areas, it is not possible to satisfy the atmospheric evaporative demand during the dry months, which results in precipitation values lower than the actual evapotranspiration. Soil
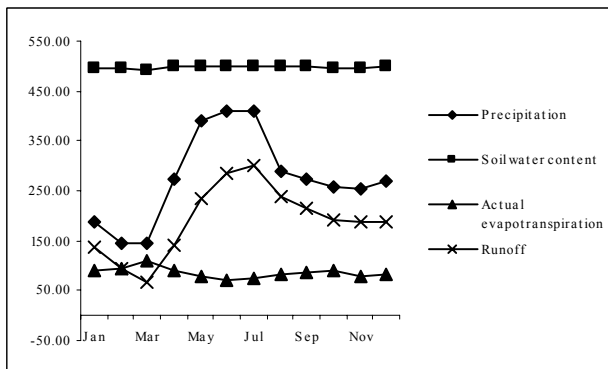

Figure 9: Mean monthly water balance components for a selected grid cell with forest cover
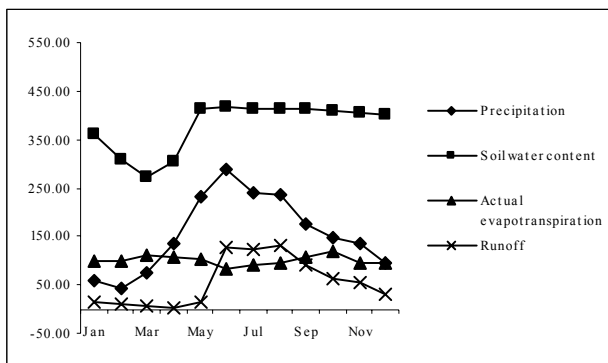

Figure 10: Mean monthly water balance components for a selected grid cell with savanna cover

moisture and surface runoff are both decreasing during the dry periods.

5.4 Land cover change impacts and El Niño scenario on the basin water balance

A hypothetical change of the vegetation cover considering a total conversion of forest to savanna is of up most scientific concern in a region where savanna areas have increased as a consequence of fire intensification, deforestation and human activities. It has also been reported that an "El Niño" situation coincides with a decrease in the precipitation and lower peak flows as occurred during El Niño events of 1982-83 and 1998-99 (Cárdenas et al., 2003).

To investigate the impacts of these conditions on the components of the water balance, the WBM model was run by considering a savanna vegetation cover for the whole region, a climate situation as during El Niño 1982-83 and the long term climate and actual vegetation conditions (base scenario). These results are presented in Figure 11. During the scenario "El Niño" the total

annual precipitation is 2715 mm/year in comparison with 2871 mm/year for the long term mean. While the soil water content is similar for the three scenarios, the actual evapotranspiration is reduced considerably (from 1214 mm/year to 139 mm/year in both cases). These reductions are traduced in an increase of surface runoff from 1656 mm/year on the base scenario to 2731 mm/year for the savanna scenario and 2576 mm/year for the "El Niño" scenario. For the savanna scenario no attempt was done to consider possible changes in precipitation as induced by the land cover change.

The runoff coefficient curves were calculated for the three scenarios: "long term", "savanna" and "El Niño". One can observed very similar curves for the savanna and El Niño scenarios in where approximately 80% of precipitation is transformed to runoff disregarding the precipitation level. This behavior although indicative of a higher basin water production on average, can have negative impacts on the sediment transport of the rivers, affecting considerably the life time of the existing dam system for hydropower generation.
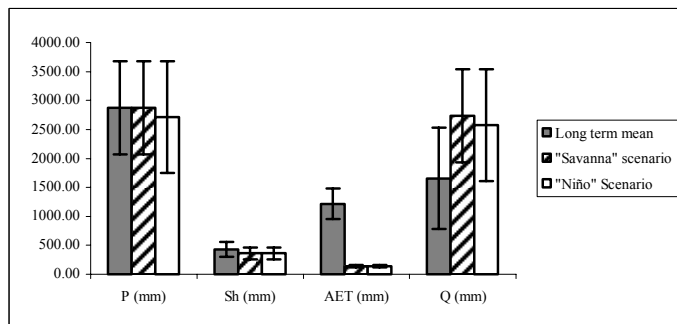

Figure 11: Mean annual values of the water balance components under different scenarios (P=Precipitation; Sh=Soil water content; AET: Actual evapotranspiration; Q: Surface runoff)
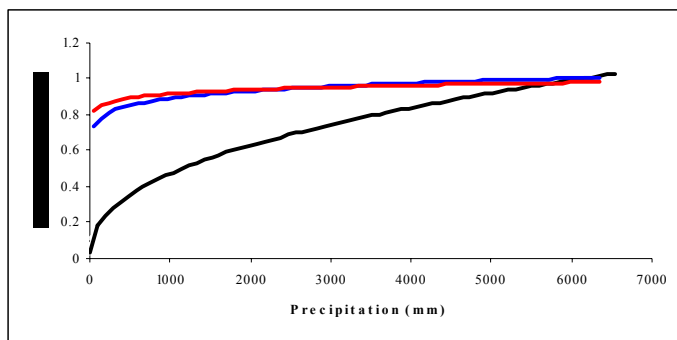

Figure 12: Runoff coefficients for three different scenarios: Long term base scenario (black), savanna scenario (red) and El Niño scenario (Blue).

6.CONCLUSIONS

The high precipitation conditions of the Caroní river basin are enough to satisfy the evaporative demand of the cathment and to keep the soil water content close to field capacity for most of the year with a mean surface runoff production of 1,656 mm/year. However changes in vegetation cover by the conversion of forest to savanna areas, do affect its water regime by lowering actual evapotranspiration and increasing surface water production. This apparent positive condition might bring negative consequences by increasing the basin sediment yield, especially if deforestation and human activities continue to increase at the actual rate. These results demonstrate the forests regulating role in the evaporative processes and final water production of the catchment. On drier conditions as the one of El Niño 1982-1983 situation, a similar catchment response than the forest to savanna conversion was observed. The spatial and temporal distribution of precipitation under such conditions may also jeopardize the forest regulating role. This point deserves more investigation for which it is important to study in more detail the spatial effect of El Niño conditions across the region.

7. ACKNOWLEDGMENTS

8. REFERENCES

Arnell, N. W. 1999. A simple water balance model for the simulation of streamflow over a large geographic domain. Journal of Hydrology, 217: 314-335.

ArcView GIS 3.2 system (ESRI, 1992-1999).

Cárdenas, P., M. Martelo, L. García y A. Gil. 2003. Impacto de los eventos El Niño – Oscilación del Sur en Venezuela. Parte II. Reporte presentado a la Comisión Andina de Fomento. 208 pp.

Corporación Venezolana de Guayana (CVG); Técnica Minera C. A. (TECMIN), Gerencia de Proyectos Especiales. 1987. "Inventario de los Recursos Naturales Región Guayana (RENAGUA): Mapa de Suelo". Ciudad Bolívar, Venezuela. Mapa a escala 1:250.000

Dezzeo, N. (ed), 1994, Ecología de la altiplanicie de la Gran Sabana (Guayana Venezolana). I. Investigaciones sobre la dinámica bosque-sabana en el sector SE: subcuencas de los ríos Yuruaní, Arabopó y Alto Kukenán, Scientia Guaianae , 4, xxxviii, 205 pp.

Döll, P.; F. Kaspar y B. Lehner. 2003. A global hydrological model for deriving water availability indicators: model tuning and validation. Journal of Hydrology, 270: 105-134.

EDELCA. 2001. Cifras. [On line]. http://www.edelca.com.ve/

Eva, H.D., Miranda, E.E. de, Di Bella, C.M. Gond., V. Et al., 2002. A Vegetation Map of South America, EUR 20159 EN, European Commission, Luxembourg.

Federer, C.A., C. Vörösmarty, and B. Fekete. 2003. Sensitivity of annual evaporation to soil and root properties in two models of contrasting complexity. J. Hydrometeorology 4:1276-1290.

Federer, C. A.; C. Vörösmarty y B. Fekete. 1996. Intercomparison of methods for calculating potential evaporation in regional and global water balance models. Water Resources Research, 32(7): 2315-2321.

Fisher, J.B., T.A. DeBiase,Y. Qi, M. Xu, and A.H.Goldstein. 2005. Evapotranspiration models compared on a Sierra Nevada forest ecosystem, Environmental Modelling and Software 20: 783-796.

Guenni, L; Sanso,L.; Betancourt,L. 2002. "Oceanic influence on the precipitation os the south-east of Venezuela". Environmetrics, 13: 263 – 279.

Huber, O., 1986, "La vegetación de la Cuenca del Río Caroní", Interciencia , 11, 301-310.

Hulme M, Mitchell JFB, Jenkins J, Gregory JM, New M,Viner D (1999) Global climate scenarios for fast-trackimpacts studies. Glob Env Change Suppl Iss:S3–S19.

Hutchinson, M. 2002. ANUSPLIN Version 4.2 User guide. Center for Resource and Environmental Studies, Canberra. The Australian National University. 52 pp.

Idrisi 3.2 Release Two (Clark Labs., 1994-2002).

Kingsbury, N. D. 2001. Impacts of land use and cultural change in a fragile environment: indigenous acculturation and deforestation in Kavanayén, Gran Sabana, Venezuela.

Millennium Ecosystem Assessment, 2003. Ecosystems and Human Well-Being. World Resources Institute, Island Press. Washington, 212 pp.

Marengo, J. 2004. Interdecadal variability and trends of rainfall across the Amazon basin. Theoretical and applied climatology, 78: 79 – 96.

New M., D. Lister, Hulme M. and I. Makin. 2000. A high-resolution data set of surface climate over global land areas. Climate Research, 21: 1-25

Poveda, G. y O. J. Mesa. 1997. Feedbacks between hydrological processes in tropical South America and Large-Scale Ocean-Atmospheric Phenomena. Journal of Climate, 10: 2690-2702.

Schmidt, P. 2004. Application of the COSERO-Model in the Caroní Basin, Venezuela. Universität Für Bodenkultur. Institut Für Wasserwirtschaft, Hydrologie und Konstruktiven Wasserbau. Wien. 156 pp.

Vörösmarty, C. J.; C. J. Wilmott; B. J. Choudhury; A. L. Schloss; T. K Stearns; S. M. Robeson y T. J. Dorman. 1996. Analyzing the discharge regime of a large tropical river through remote sensing, ground-based climatic data, and modeling. Water Resources Research, 32: 3137-3150.

Vörösmarty,C. J., C. A. Federer y A.L. Schloss. 1998. Potential evaporation functions compared on US watersheds: Possible implications for global-scale water balance and terrestrial ecosystem modeling. Journal of Hydrology, 207:147-169.

Vörösmarty,C. J.; B. Moore III; A. L. Grace; M. P. Gildea; J. M. Melillo; B. J. Peterson; E. B. Rastetter y P. A. Steudler. 1989. Continental scale models of water balance and fluvial transport: an application to South America. Global Biochemical Cycles, 3(3): 241-265.

Yates, D. N. 1997. Approaches to continental scale runoff for integrated assessment models. Journal of Hydrology, 201: 289-310.

APPENDIX A

WBM model Equations (Adapted from Vörösmarty et al., 1998)

The WBM simulates soil moisture variations, evapotranspiration, and runoff on single grid cells using biophysical data sets that include climatic drivers, vegetation, and soil parameters. The state variables are determined by interactions among time-varying precipitation, potential evaporation, and soil water content. The original model has been described in detail by Vörösmarty and coworkers (Vörösmarty et al. 1989, Vörösmarty et al. 1996, Vörösmarty and Moore 1991). The governing equations can be summarized as follows:

Equation variables:

dW_s/dt	change in soil moisture
p	probability that a day has a wetting event
P_a	available precipitation (rainfall and snowmelt) [mm day^{-1}]
$g(W_s)$	unitless soil drying function
E_p	potential evaporation [mm day^{-1}]
D_{ws}	soil moisture deficit equal to amount of water required within a time step to fill soil to its water holding capacity and simultaneously satisfy potential evaporation [mm day^{-1}]
E_a	actual evapotranspiration [mm day^{-1}]
X_r	excess rainfall (available for runoff and runoff detention pool) [mm day^{-1}]
P_r	rainfall
W_s	soil moisture [mm]

Change in soil moisture

$$
\begin{aligned}
dW_s/dt &= -g(W_s)(E_p - P_a) & P_a < E_p \\
&= P_a - E_p & E_p < P_a < D_{ws} \\
&= D_{ws} - E_p & D_{ws} < P_a
\end{aligned}
$$

Estimated actual evapotranspiration

E_a $= P_a - dW_s/dt$ $\qquad P_a < E_p$

$\quad$ $= E_p$ $\qquad\qquad\quad$ $E_p < P_a$

Excess rainfall available for runoff and recharge of runoff detention pools

X_r $= 0$ $\qquad\qquad\quad$ $P_a < D_{ws}$

$\quad$ $= P_r - D_{ws}$ $\qquad\quad$ $D_{ws} < P_a$

The unitless drying function

Equation variables:

α $\qquad\qquad\qquad$ empirical constant

W_s $\qquad\qquad\qquad$ soil moisture [mm]

W_c $\qquad\qquad\qquad$ soil and vegetation-dependent available water capacity [mm]

$g(W_s)$ $= 1 - e^{(-\alpha W_s/W_c)} / 1 - e^{-\alpha}$

$\alpha = 5.0$ so that the drying curve would resemble that of Pierce (1958) when $g(W_s) = E_a/E_p$ is plotted as a function of W_s/W_c during periods of no precipitation.

Wetting Event Probability

Equation variables:

p $\qquad\qquad\qquad$ probability that a day has a wetting event

P_{rm} $\qquad\qquad\qquad$ monthly rain

$p = \alpha(1 - e^{-\beta(Prm)})$

, $\qquad\qquad\qquad$ Parameters changing with geographic location

Precipitation available for soil recharge as rainfall

Equation variables:

P_r $\qquad\qquad\qquad$ rainfall

P_{rm} $\qquad\qquad\qquad$ monthly rain

n_d number of days in a month

$P_r = P_{rm}/n_d p$

.

Rainfall derived Runoff

Equation variables:

D_r $\qquad\qquad\qquad$ rainfall runoff detention pool

R_r $\qquad\qquad\qquad$ rainfall-derived runoff emerging from the grid cell

X_r $\qquad\qquad\qquad$ excess rainfall (available for runoff and runoff detention pool) [mm day^{-1}]

β and γ $\qquad\qquad$ empirical constants set to 0.0167 [day^{-1}] and 0.5 respectively

$dD_r/dt = (1 - \gamma) X_r - \beta D_r$

$R_r = \gamma X_r + \beta D_r$

The expected monthly changes in the pools are calculated as the average daily change multiplied by n_d, the number of days in each month. Likewise, the associated water fluxes computed by the WBM are initially expressed as a daily average for the duration of each month. These also are multiplied by n_d to obtain corresponding monthly values. The time varying changes in W_s, K_s, D_r and D_s are solved using a fifth-order Runge-Kutta integration technique (International Mathematical and Statistical Libraries, Houston TX).